MOLECULAR AND CELLULAR BIOLOGY, Nov. 2008, p. 6858–6869 Vol. 28, No. 22
0270-7306/08/$08.00+0 doi:10.1128/MCB.00367-08

Autophosphorylation-Induced Degradation of the Pho85 Cyclin Pcl5 Is Essential for Response to Amino Acid Limitation▽

Sharon Aviram,[1]† Einav Simon,[1] Tsvia Gildor,[1] Fabian Glaser,[2] and Daniel Kornitzer[1]*

Department of Molecular Microbiology, B. Rappaport Faculty of Medicine, Technion–I.I.T. and the Rappaport Institute for Research in the Medical Sciences, Haifa 31096, Israel,[1] and Bioinformatics Knowledge Unit, The Lorry I. Lokey Interdisciplinary Center for Life Sciences and Engineering, Technion–I.I.T., Haifa 32000, Israel[2]

Received 4 March 2008/Returned for modification 18 April 2008/Accepted 15 August 2008

Pho85 cyclins (Pcls), activators of the yeast cyclin-dependent kinase (CDK) Pho85, belong together with the p35 activator of mammalian CDK5 to a distinct structural cyclin class. Different Pcls target Pho85 to distinct substrates. Pcl5 targets Pho85 specifically to Gcn4, a yeast transcription factor involved in the response to amino acid starvation, eventually causing the degradation of Gcn4. Pcl5 is itself highly unstable, an instability that was postulated to be important for regulation of Gcn4 degradation. We used hybrids between different Pcls to circumscribe the substrate recognition function to the core cyclin box domain of Pcl5. Furthermore, the cyclin hybrids revealed that Pcl5 degradation is uniquely dependent on two distinct degradation signals: one N-terminal and one C-terminal to the cyclin box domain. Whereas the C-terminal degradation signal is independent of Pho85, the N-terminal degradation signal requires phosphorylation of a specific threonine residue by the Pho85 molecule bound to the cyclin. This latter mode of degradation depends on the SCF ubiquitin ligase. Degradation of Pcl5 after self-catalyzed phosphorylation ensures that activity of the Pho85/Pcl5 complex is self-limiting in vivo. We demonstrate the importance of this mechanism for the regulation of Gcn4 degradation and for cell growth under conditions of amino acid starvation.

Cyclin-dependent kinases (CDKs) are central cellular regulators that are involved in cell proliferation (46), as well as other processes, e.g., regulation of transcription via the phosphorylation of RNA polymerase II (7). CDKs are activated by binding of an ancillary subunit, the cyclin (32, 44). The cyclins also participate in targeting the kinase to specific substrates (28, 55, 65; reviewed in reference 43). Cyclins were so named because of their cyclic appearance and disappearance from the cells, in correlation with cell cycle progression (16). Their rapid and coordinated disappearance depends on the ubiquitin system, with the anaphase-promoting complex/cyclosome ubiquitin ligase being responsible for targeting mitotic cyclins, and SCF-type ubiquitin ligases often being involved in the degradation of G1 cyclins (68). However, not all cyclins are directly involved in cell cycle regulation, and not all cyclins are unstable. Common to all cyclins is that they possess a region of moderate sequence conservation, the cyclin box. The cyclin box was shown to assume a typical five-helix structure (8, 32), with helix 5 contacting the CDK near its catalytic site and helix 1 facing away from the CDK (32).

The yeast CDK Pho85, a regulator of cell morphogenesis and of several metabolic pathways, is structurally and functionally related to the mammalian kinase CDK5 (29, 48). Of 10 Pho85 cyclin (Pcl) paralogs identified in yeast (40), many were associated with the phosphorylation of specific target proteins (reviewed in references 10 and 27). The role of the cyclin in target selectivity is further underscored by the observation that even the specificity of Pcl orthologs can coevolve with their protein target (19).

The Pcl Pho80 is required for the phosphorylation of the transcription factor Pho4 by Pho85 (34). The recently obtained crystal structure of the Pho85/Pho80 complex indicated that Pho80 is structurally distinct from other cyclins, and more similar in structure to p35, an activator of CDK5 that shows very limited sequence homology to other cyclins (30). Unlike the typical double cyclin box configuration of most cyclins, Pho80, like p35, contains a single core 5 α-helix cyclin box domain, with one additional α-helix N-terminal and two additional α-helices C-terminal to the core structure (30, 60).

A distinct Pho85 cyclin, Pcl5, is required for phosphorylation of the bZIP transcription factor Gcn4 by Pho85 (41, 56). Gcn4 was initially characterized as being involved in the pathways of biosynthesis of amino acids and purine samples (23, 25) and more recently was shown to regulate a significant proportion of the yeast genes (47). Under standard growth conditions Gcn4 is degraded very rapidly, but it is stabilized under conditions of amino acid limitation or of partial inhibition of protein synthesis (37, 41). Degradation of Gcn4 depends on its phosphorylation at a specific residue, Thr165, by Pho85/Pcl5 (41), which leads to its ubiquitination by the ubiquitin-conjugating enzyme Cdc34 (37) in conjunction with the ubiquitin ligase SCF^{CDC4} (11, 41).

Cyclins themselves are often rapidly degraded via the ubiquitin-proteasome system (68). Pcls appear to fall into two classes: one of stable cyclins ($t_{1/2} > 10$ min: e.g., Pcl6, Pcl7, Pcl8, and Pho80) and one of unstable cyclins ($t_{1/2} < 5$ min: e.g., Pcl1, Pcl2, and Pcl5) (3, 56; our unpublished results). With regard to

* Corresponding author. Mailing address: Department of Molecular Microbiology, B. Rappaport Faculty of Medicine, 2 Efron St., Haifa 31096, Israel. Phone: 972-4-829 5258. Fax: 972-4-829 5254. E-mail: danielk@techunix.technion.ac.il.

† Present address: University of Texas Southwestern Medical Center, Dallas, TX 75390-9185.

▽ Published ahead of print on 15 September 2008.

Pcl5, it was hypothesized that its extremely short half-life—on the order of 2 to 3 min under both sated and amino acid starvation conditions—may be intimately linked to its regulatory role in amino acid biosynthesis and may explain the starvation-dependent regulation of Gcn4 degradation (56): under conditions of starvation or reduced protein synthesis, Pcl5 degradation would not be balanced by new protein synthesis, causing it to rapidly disappear from the cells, thereby leading to Gcn4 stabilization.

To test this notion, we set out here to characterize the mechanism of Pcl5 degradation. Since, in contrast to other types of cyclins, nothing is known about the degradation pathway of the unstable Pcls, we adopted an approach based on the construction of hybrids between Pcl5 and the stable Pcl Pho80. The hybrid cyclins enabled us to circumscribe the substrate specificity region of Pcl5 to the central cyclin box domain and to identify two distinct degradation signals, within the C- and N-terminal domains of Pcl5. The C-terminal degradation signal (CDS) functions independently of the rest of the protein, whereas the N-terminal degradation signal (NDS) requires phosphorylation in *cis* by the bound Pho85 molecule, making it highly dependent on Pcl5/Pho85 activity and on protein levels. The characterization of the Pcl5 degradation signals enabled us to construct a stabilized Pcl5 mutant, allowing us to test the role of rapid Pcl5 turnover in the regulation of Gcn4 degradation and in the cellular response to amino acid starvation.

MATERIALS AND METHODS

Saccharomyces cerevisiae strains and growth conditions. All experiments were performed with *S. cerevisiae* strain W303 (R. Rothstein) or BY4741 (EUROSCARF). Strains KY546 (*pho85*Δ) and KY827 (*pcl5*Δ) were described previously (41, 56). Strain KY1114 is BY4741 *pho85*Δ::Kan^r (EUROSCARF). Strain KY1137 was constructed by integrating the Myc_{13} Kan^r cassette (39) to the 3′ end of the *PCL5* open reading frame of W303. KY1185 is KY1137 *pho85*Δ::*LEU2* (*PHO85* disrupted with a *pho85*Δ::*LEU2* cassette provided by B. Andrews). The W303 *cdc53-1*, *cdc34-2* and *cdc4-1* mutant strains were provided by M. Tyers, and the *grr1*Δ strain and other F-box protein deletion strains were obtained from EUROSCARF.

The strains were grown in standard yeast extract-peptone-dextrose (YPD; 1% yeast extract, 2% peptone, 2% dextrose) and complete yeast nitrogen base (YNB; 1.5 g of yeast nitrogen base/liter, 5 g of ammonium sulfate/liter, 2% dextrose or galactose, 0.1 g of each amino acid, uracil and adenine/liter, with the appropriate amino acids removed as required for plasmid selection) media.

Plasmid constructions. The plasmids used in the present study are listed in Table 1. KB1030 was constructed in two steps: first, the EcoRI-XhoI Gcn4(62-202)-Myc_3 fragment of KB891 (41) was cloned into p416GALL (45); then, the EcoRI-XbaI Gcn4(62-202) fragment of the resulting plasmid was replaced with a *PCL5* PCR fragment. KB1298 to KB1301, KB1324, and KB1360 were constructed by ligating or fusing PCR fragments that were then cloned as BamHI-XhoI fragments into p416-GAL1 (45). KB1298 carries *PCL5* nucleotide coordinates 1 to 534 and *PHO80* coordinates 508 to 882 with a SacI site at the interface. KB1299 carries *PCL5* (coordinates 1 to 309) and *PHO80* (coordinates 301 to 882) with a ClaI site at the interface. KB1300 carries *PHO80* (coordinates 1 to 309) and *PCL5* (coordinates 316 to 690) with a ClaI site at the interface. KB1301 carries *PHO80* (coordinates 1 to 504) and *PCL5* (coordinates 535 to 690) with a SacI site at the interface. KB1324 carries *PHO80* (coordinates 1 to 219) *PCL5* (coordinates 235 to 690) (P5/P2) spliced together with a bridging oligonucleotide. KB1360 was obtained by ligating *PHO80* (coordinates 1 to 219) *PCL5* (coordinates 235 to 528) amplified from KB1324, to *PHO80* (coordinates 508 to 882), with a SacI site at the interface. KB1595 consists of pRS313 carrying the *PCL5* promoter, coordinates −890 to −3, as a HindIII-XbaI fragment fused to the Pho80-Pcl5-Pho80 hybrid of KB1360 amplified as an SpeI-XhoI fragment. KB1169, KB1338, KB1339, and KB1348 were built by fusion of PCR fragments carrying the indicated regions of Pcl5 (Table 1) downstream of the *URA3* gene of pOC9 (20). KB1716 and KB1718 were constructed by fusing the promoter region of *PCL5* from position −884, to the open reading frame (either wild type or T32A) from position 15, introducing an artificial XbaI site and changing residue 5 of Pcl5 from His to Leu. The fused fragment was cloned into pRS313 (57). KB1222 and KB1236 were generated by site-directed mutagenesis of the PCL5 gene of KB1093. KB1448 was generated by introducing CUP1::PCL5 SacI-XhoI from KB1269 into pRS313 (57). KB1604 was generated by fusing the PCL5 T32A PCR fragment of KB1222 using MfeI-XhoI into KB1591 (pRS313 inserted with CUP1 SacI-RI)-cut RI-XhoI. KB1739 and KB1741 carry the PCL5 and PCL5 T32A alleles fused to Myc_{13}, using a BamHI site found at the 5′ end of the Myc_{13} cassette (39), and a primer to introduce a BamHI site at the 3′ end of the *PCL5* open reading frame. KB1740 was isolated as a spontaneous mutant in the course of constructing KB1739. KB1108 was constructed by introducing

TABLE 1. Plasmids used in this study

Plasmid	Description	Source or reference
EB0092	GPDp-*HA-PHO80* 2μm *URA3*	34
pGEX-PHO85	TACp-*GST-PHO85*	49
KB823	*GAL1-GST-PHO85* 2μm *URA3*	49
KB1106	T7p-His_6-*PCL5*	56
KB1802	T7p-His_6-*PCL5*(*L158P*)	This study
KB161	*GAL1-GCN4* 2μm *URA3*	37
KB843	*GAL1-GCN4 CEN TRP1*	41
KB1093	GAL1p-$PCL5_{aa1-229}$ *CEN URA3*	56
KB1773	GAL1p-$PCL5_{aa41-229}$ *CEN URA3*	This study
KB1774	GAL1p-$PCL5_{aa71-229}$ *CEN URA3*	This study
KB1030	GAL1p-*PCL5*-Myc_3 *CEN URA3*	This study
KB1298	GAL1p-$PCL5_{aa1-178}$-$PHO80_{aa170-294}$ *CEN URA3*	This study
KB1299	GAL1p-$PCL5_{aa1-103}$-$PHO80_{aa101-294}$ *CEN URA3*	This study
KB1300	GAL1p-$PHO80_{aa1-103}$-$PCL5_{aa106-229}$ *CEN URA3*	This study
KB1301	GAL1p-$PHO80_{aa1-170}$-$PCL5_{aa178-229}$ *CEN URA3*	This study
KB1324	GAL1p-$PHO80_{aa1-73}$-$PCL5_{aa79-229}$ *CEN URA3*	This study
KB1331	GAL1p-$PHO80_{aa1-294}$ *CEN URA3*	This study
KB1360	GAL1p-$PHO80_{aa1-73}$-$PCL5_{aa79-178}$-$PHO80_{aa170-294}$ *CEN URA3*	This study
KB1595	PCL5p-$PHO80_{aa1-73}$-$PCL5_{aa79-178}$-$PHO80_{aa170-294}$ *CEN HIS3*	This study
pOC9	CUP1p-*URA3 CEN TRP1*	20
KB1169	CUP1p-*URA3-PCL5 CEN TRP1*	This study
KB1338	CUP1p-*URA3*-$PCL5_{aa174-229}$ *CEN TRP1*	This study
KB1339	CUP1p-*URA3*-$PCL5_{aa205-229}$ *CEN TRP1*	This study
KB1448	CUP1p-*PCL5 CEN HIS3*	This study
KB1602	CUP1p-*PCL5*(*T32A*) *CEN HIS3*	This study
KB1604	CUP1p-*PCL5*(*T8A T32A T202A*) *CEN HIS3*	This study
KB1222	KB1093 *PCL5*(*T32A*)	This study
KB1236	KB1093 *PCL5*(*T8A T32A T202A*)	This study
KB1269	CUP1p-*PCL5 CEN TRP1*	This study
KB1270	KB1269 *PCL5*(*T32A*)	This study
KB1716	*PCL5 CEN HIS3*	This study
KB1718	*PCL5*(*T32A*) *CEN HIS3*	This study
KB1722	*PCL5*(*T8A T32A T202A*) *CEN HIS3*	This study
KB1739	*PCL5*-Myc_{13} *CEN HIS3*	This study
KB1740	*PCL5*(*L158P*)-Myc_{13} *CEN HIS3*	This study
KB1741	*PCL5*(*T32A*)-Myc_{13} *CEN HIS3*	This study
KB1108	ADH1p 2μm *URA3*	This study
KB1310	ADH1p-*PCL5* 2μm *URA3*	This study
KB1876	TACp-GST-Pcl5	This study
KB1877	TACp-GST-$Pcl5_{T32A}$	This study
KB1878	TACp-GST-$Pcl5_{L158P}$	This study
KB1931	GAL1p-*PCL5*-Myc_{13} *CEN HIS3*	This study
KB1932	GAL1p-*PCL5*(*T32A*)-Myc_{13} *CEN HIS3*	This study

the BamHI-EcoRI *ADH1* promoter fragment of pADHUBC2 (13) into p426GAL1 (45). A *PCL5* MfeI-XhoI PCR fragment was cloned into KB1108 digested with EcoRI and XhoI to generate KB1310. KB1773 and KB1774 consist of *PCL5* from nucleotides 121 and 211, respectively, to the termination codon, cloned as MfeI-ATG-XhoI PCR fragments into p416GAL1 (45). KB1876 and KB1878 were constructed by cloning, respectively *PCL5*, *PCL5 T32A*, and *PCL5 L158P* as BamHI-XhoI PCR fragments in-frame to the glutathione *S*-transferase (GST) sequence of plasmid pGEX-4T-1 (Pharmacia). KB1931-2 were constructed by cloning BglII-XhoI *PCL5*-Myc_{13} PCR fragments amplified from KB1739 and KB1741, respectively, into p414GAL1 (45).

Protein degradation analysis. Pulse-chase protein degradation analysis was performed as described previously (36). Briefly, cells (10 ml) were grown in synthetic dropout medium to an optical density at 600 nm (OD_{600}) of 0.7 to 1.0, spun down, washed once in the same medium lacking methionine and cysteine, resuspended in 0.3 ml of the same medium containing [^{35}S]methionine-cysteine (Express; NEN), and incubated for 5 min at 30°C. Cells were then spun down and resuspended in 2.5 ml of synthetic complete medium containing 10 mM concentrations (each) of methionine and cysteine. At the indicated times, an aliquot was removed, treated with NaOH (0.25 M) and β-mercaptoethanol (1%), incubated for 10 min on ice, and then precipitated with 7% trichloroacetic acid. The protein pellet was washed with acetone and resolubilized in 2.5% sodium dodecyl sulfate, and the target protein was immunoprecipitated from this extract using a polyclonal anti-Gcn4 (41) or anti-Pcl5 (56) antisera. To induce amino acid starvation, cells were harvested by centrifugation and grown in YNB plus adenine and uracil for 1 h before labeling and then chased in the same medium plus methionine and cysteine.

Alternatively, protein stability was assayed by monitoring the levels of specific proteins by Western blotting, after arrest of protein synthesis by addition of the protein synthesis inhibitor cycloheximide (20 μg/ml) to the medium.

Enzyme assays. (i) Acid phosphatase assay. Pho80 function was tested by measuring secreted phosphatase activity in the various strains. Under phosphate-replete conditions, Pho80 normally suppresses the expression of *PHO5*, the secreted acid phosphatase gene. In the absence of Pho80 activity, acid phosphatase activity in the medium increases. The assay protocol was based on a previously published study (62). Strain DY4659 (*pho80*) was transformed with the indicated plasmids and grown on galactose in synthetic dropout medium to late log phase. Cells from 1 ml of culture were pelleted and resuspended in 50 mM acetate buffer (pH 4.0), and 0.1 ml of *p*-nitrophenylphosphate (6.4 mg/ml) was added to the cell suspension. The reaction was carried out at 35°C until the appearance of the yellow color of the released *p*-nitrophenol and stopped by the addition of 0.5 ml of saturated Na_2CO_3. Activity units were determined as follows: (the OD_{420} of the reaction supernatant × 1,000)/(the OD_{600} of the cell suspension × the reaction time in minutes).

(ii) In vitro kinase assay. In vitro kinase assays were performed as described previously (41). Briefly, recombinant GST-Pho85 (49), GST-Pcl5 (wild type, T32A, and L158P; expressed from plasmids KB1876, KB1877, and KB1878, respectively), 10 ng (each), and 20 ng of GST-Gcn4 (expressed from KB430) (37) or 1 μg of myelin basic protein (Sigma) were mixed in a 10-μl final volume, with 1 μCi of [γ-^{32}P]ATP and 0.02 mM cold ATP. Reaction were incubated 15 min at 30°C. Pcl5 self-phosphorylation was carried out similarly, except that 1 μM cold ATP was used.

Growth tests. Yeast strains were precultured to the same optical densities (OD_{600} = 1) and spotted onto appropriate YNB media, supplemented as indicated in the figure legends. Fivefold dilutions, starting with 3×10^4 cells per 20 μl, were spotted onto the plates, incubated for 3 days at 30°C, and photographed under white light.

Pcl5 structure modeling. In order to find a homologue with a known three-dimensional structure, the Protein Data Bank (PDB) (4) was searched by using the Pcl5 sequence as a query. BLAST (1) did not yield any significant hit (data not shown); however, the HHpred tool for homology detection (59) did return several PDB entries with significant homology along the 82-182 region of the Pcl5 sequence, which includes the conserved 100 long region known as the cyclin domain or cyclin box, and only one single significant alignment that also included part of the N-terminal region (e-value 4.5e-38, sequence identity = 17%), namely, with the *S. cerevisiae* Pho80 cyclin (PDB code 2pmi, chain B), a known paralog of Pcl5, the structure of which was recently determined as part of the Pho85-Pho80 CDK-cyclin complex (30). The original automatic alignment provided by HHpred was manually corrected to allow a more accurate modeling, thus yielding a final sequence identity of 23.5% (see Fig. 1A).

To build a model structure of the Pcl5 cyclin, the MODELLER software v9.2 (15) was fed with the curated Pcl5-Pho80 alignment and the template Pho80 structure. Of the 20 Pcl5 models initially generated, the one with the lowest MODELLER objective function was chosen. Then, this best model was structurally aligned with its template (PDB 2pmi, chain B), using the MatchMaker software (42) available through the Chimera package (53). This model is depicted in complex with the Pho85 CDK structure in Fig. 9. Disordered domains and hinge regions were predicted by using the metaPrDos (31) and HingeMaster (17) servers, respectively.

RESULTS

Mapping of the substrate recognition site on Pcl5. In order to distinguish between regions of Pcl5 involved in specificity for its substrate, Gcn4, and regions required for degradation of Pcl5, we constructed hybrids of Pcl5 with Pho80. Pho80 recognizes a distinct substrate, Pho4 (24, 34), and, unlike Pcl5, it is largely stable (3) (see also Fig. 2). In order to align to protein sequences toward hybrid construction, the position of the cyclin box and of its individual helices was initially predicted from alignment of the protein sequences along with that of the sequence of cyclin A, the structure of which is known (8), as well as from secondary structure predictions using the PSIPRED method (33). The two methods yielded very similar predictions regarding the positions of the core cyclin box and its five helices. The cyclin box of Pcl5 was predicted to extend from positions 79 to 178 and that of Pho80 from positions 74 to 169. The recently published crystal structure of the Pho80-Pho85 complex (30) shows that the core cyclin box extends between residues 76 and 165, indicating that, at least for Pho80, the prediction was quite accurate. Figure 1A gives an alignment of the central regions of Pcl5 and Pho80, including the cyclin box and part of the N-terminal and C-terminal regions. The two proteins were spliced before predicted helix 1, within helix 2, or after helix 5 of the cyclin box (Fig. 1A). Pho80 activity was monitored by measuring the activity of secreted acid phosphatase, which is normally repressed in the presence of active Pho80 (67). As is shown in Table 2, none of the hybrid proteins were able to significantly suppress acid phosphatase secretion, i.e., carried Pho80 activity. Pcl5 activity was monitored by the ability of the hybrid cyclins to induce Gcn4 degradation and to suppress Gcn4 overexpression toxicity (41, 56) (high overexpression of *GCN4* inhibits cellular growth, possibly by the interference of Gcn4 with other transcriptional activation pathways [61]). Hybrids that contain the full cyclin box of Pcl5 with, in addition, either its C terminus or its N terminus (KB1298 and KB1324), as well as a hybrid carrying only the predicted cyclin box of Pcl5, but the C and N termini of Pho80 (KB1360), were able to suppress the toxicity of Gcn4 overexpression (Fig. 1B; summarized in Table 2). Since Pcl5 was shown to function in the pathway of Gcn4 degradation via the SCF^{CDC4} ubiquitination complex (41, 56), the ability of the hybrid cyclins to promote Gcn4 degradation was also assayed by pulse-chase analysis. The Gcn4 band remaining at 0, 5, and 15 min after the chase was quantitated. As can be seen in Fig. 1C, the same hybrids that were able to suppress Gcn4 toxicity were also active in the Gcn4 degradation pathway. This strongly suggests that the substrate specificity of Pcl5 is encoded within its core, 5-helix cyclin box domain. To further identify the region of the cyclin box responsible for substrate recognition, we also tested hybrids that only contain predicted helix 1 and half of helix 2, or helices 2 to 5, of Pcl5 (KB1299 and KB1300, respectively). However, these hybrid proteins were inactive, suggesting either that more than one helix is

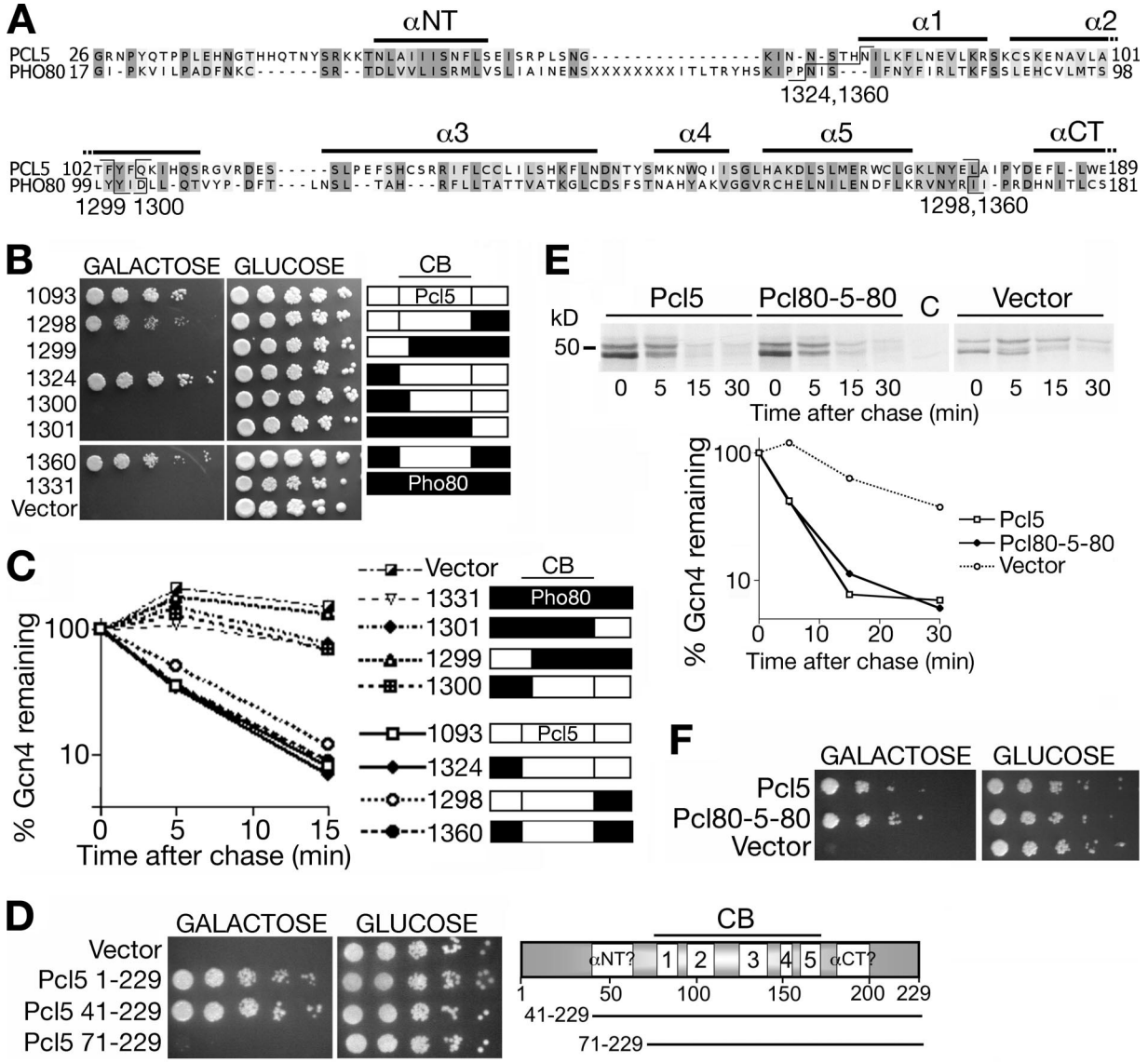

FIG. 1. Activity of Pcl5/Pho80 hybrid cyclins. (A) Sequence alignment of Pcl5 and Pho80. The initial alignment was obtained with HHpred (59) and manually curated. The position of the helices of the cyclin box (α1 to α5) and of the αNT and the start of the αCT1 helix are based on the Pho80 crystal structure (30). The position of the fusions that generated the Pcl hybrids are indicated with the number of the corresponding plasmids. Plasmid KB1301 is the exact reverse of KB1298. (B) The *pcl5*Δ strain KY827 carrying plasmid KB843 (*GAL1-GCN4*) was transformed with the indicated hybrid cyclin-expressing plasmids. Dilutions of the cell suspensions were spotted on synthetic complete drop-out plates with galactose (inducing conditions) or glucose (repressing conditions) as indicated and photographed after 3 and 2 days, respectively, of growth at 30°C. (C) The same cultures were used to measure Gcn4 stability by pulse-chase analysis, followed by immunoprecipitation (see Materials and Methods). The Gcn4 band remaining at each time point was quantitated with a phosphorimager. (D) The *pcl5*Δ strain KY827 carrying plasmid KB843 (*GAL1-GCN4*) was transformed with full-length and N-terminal truncations of Pcl5, as indicated, expressed from plasmids KB1093, KB1773, and KB1774. Dilutions of the cell suspensions were spotted and grown as for panel B. On the left, a schematic representation of the Pcl5 sequence, with the position of the predicted α-helices according to panel A. (E) The natively expressed Pho80-Pcl5-Pho80 hybrid induces Gcn4 degradation. A *pcl5*Δ strain expressing *GCN4* from the *GAL1* promoter of plasmid KB161 (37) was cotransformed with either a vector plasmid, a plasmid (KB1594) carrying the wild-type *PCL5* gene, or plasmid KB1595, expressing the Pho80-Pcl5-Pho80 hybrid from the *PCL5* promoter, as indicated. Gcn4 degradation was followed by pulse-chase analysis. C, no-tag control. (F) The natively expressed Pho80-Pcl5-Pho80 hybrid suppresses toxicity of Gcn4 overexpression. The same strains analyzed in panel E were grown and tested for Gcn4 overexpression toxicity as described in panel B.

involved in substrate recognition or that the structure of the protein was disrupted in these constructs.

The Pho80 structure includes, in addition to the core 5-helix cyclin box, two extra C-terminal α-helices and one extra N-terminal α-helix (αNT), the latter extending between residues 34 and 50 of Pho80 (30). Secondary structure prediction (33) indicated the presence of a similar extended α helix in Pcl5 between residues 41 and 64, of which residues 52 to 62 may align with the Pho80 αNT. The active Pho80/Pcl5 hybrids carry the 5-helix cyclin box of Pcl5, but the αNT helix region of Pho80 instead of the corresponding region of Pcl5. We tested whether this region of Pcl5 is at all important for activity by

TABLE 2. Summary of Pcl5/Pho80 hybrids activity and stability[a]

Plasmid	N terminus	Cyclin box	C terminus	Gcn4 $t_{1/2}$ (min)	Suppression of Gcn4 toxicity	Acid phosphatase activity	Cyclin $t_{1/2}$ (min)
KB1093	Pcl5	Pcl5	Pcl5	3	+	NA	2.5
KB1298	Pcl5	Pcl5	Pho80	5	+	327	10
KB1299	Pcl5	Pcl5 (helix 1) Pho80 (helices 2 to 5)	Pho80	>15	–	286	10
KB1324	Pho80	Pcl5	Pcl5	3	+	271	3.5
KB1300	Pho80	Pho80 (helix 1) Pcl5 (helices 2 to 5)	Pcl5	>15	–	315	5
KB1301	Pho80	Pho80	Pcl5	>15	–	353	5
KB1360	Pho80	Pcl5	Pho80	3	+	NA	>15
KB1331	Pho80	Pho80	Pho80	>15	–	30	>30†
Vector				>15	–	444	

[a] Summary of the activities and stabilities of the various Pcl5/Pho80 hybrids expressed from the *GAL1* promoter of the indicated plasmids. Suppression of Gcn4 toxicity is shown in Fig. 1B. The half-life of Gcn4 is derived from the decay curves shown in Fig. 1C. Cyclin half-lives are derived from the decay curves shown in Fig. 2. Acid phosphatase activity was measured as described in Materials and Methods. †, the Pho80 half-life was measured using the HA-Pho80 construct of plasmid EB0092 rather than the untagged Pho80 of plasmid KB1331. NA, not applicable.

constructing two N-terminal truncations: one starting at position 41 and one at position 71 of the Pcl5 sequence. Both truncations were placed under the *GAL1* promoter and were tested for their ability to suppress Gcn4 overexpression toxicity as described above. The results shown in Fig. 1D indicate that, whereas the truncation starting at position 41 was as active as the full-length protein, if not more so, the truncation starting at position 71 was completely inactive, suggesting that the region of Pcl5 corresponding to the Pho80 αNT helix is essential for activity but can be replaced by the homologous Pho80 region.

In the activity assays with the hybrid cyclins shown above, the proteins were overexpressed under the strong *GAL1* promoter, raising the concern that the active Pcl hybrids are in fact only able to complement Pcl5 activity because of their artificially high levels. To eliminate this possibility, the most informative hybrid, containing the N and C termini of Pho80 and the cyclin box of Pcl5, or Pcl80-5-80 (plasmid KB1360), was cloned under the natural *PCL5* promoter. This construct was able to complement the *pcl5*Δ mutant for Gcn4 degradation (Fig. 1E). Quantitation of this experiment showed that both Pcl5 and the 80-5-80 hybrid induced Gcn4 degradation with a half-life of about 4 min compared to a more than 20-min half-life for Gcn4 in the *pcl5*Δ mutant (56). Furthermore, based on the Gcn4 toxicity overexpression assay, this hybrid appeared to be at least as active as native *PCL5* (Fig. 1F). These data indicate that the specific activity of Pcl5 toward Gcn4 can be fully accounted for by the core cyclin box domain only.

Mapping of the degradation signal on Pcl5. Pcl5 is rapidly degraded, with a half-life of <3 min (56). Since degradation signals are often *cis* dominant, i.e., will confer degradation when fused to a normally stable protein, and since we found that the Pho80 cyclin is stable (Fig. 2), we took advantage of the Pcl5/Pho80 hybrids to attempt to locate the Pcl5 degradation signal(s). The stability of the various Pcl5/Pho80 hybrids was assayed by pulse-chase analysis of the hybrid cyclins overexpressed from the *GAL1* promoter. As shown in Fig. 2, both the N-terminal and the C-terminal domains of Pcl5 were individually able to confer degradation to the stable Pho80 cyclin, indicating the presence of two degradation signals in Pcl5, one in each of these two domains. Conversely, KB1360—the Pcl80-5-80 hybrid protein—was stable, suggesting that the cyclin box domain of Pcl5 does not carry a degradation signal. Half-lives of the hybrid proteins indicate that the C-terminal signal alone is able to account for most of the degradation of Pcl5 (plasmids KB1300, KB1301, and KB1324), whereas the N-terminal domain alone causes the hybrid proteins to be degraded with half-lives of 10 to 15 min (plasmids KB1298 and KB1299), i.e., significantly shorter than that of Pho80, but not as short as that of native Pcl5.

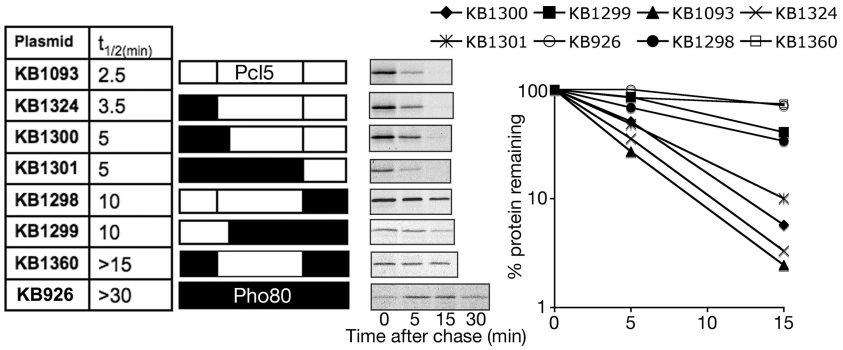

FIG. 2. Stability of Pcl5/Pho80 hybrid cyclins. The stability of the various hybrids, expressed from the inducible *GAL1* promoter, was measured by pulse-chase analysis using a polyclonal anti-Pcl5 antiserum, except for Pho80, for which a hemagglutinin (HA)-tagged version was followed using the anti-HA monoclonal antibody. The structure of the hybrid cyclins is shown schematically. See Table 1 for the precise coordinates of the cyclin fragments in each hybrid.

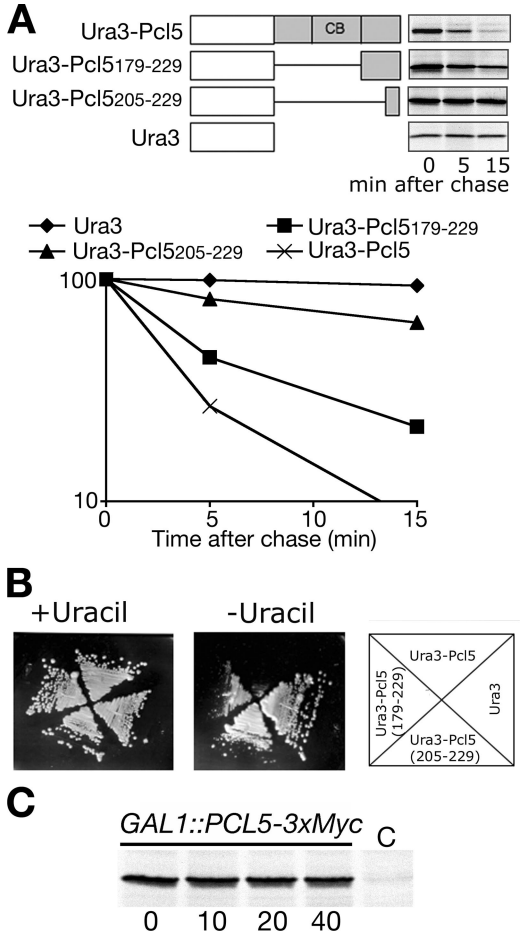

FIG. 3. CDS of Pcl5. (A) Full-length or N-terminal deletions of Pcl5 were fused to the C terminus of Ura3, as indicated, and expressed from the *CUP1* promoter of plasmids KB1169, KB1338, KB1339, and KB1348, respectively. Degradation of the fusion proteins was measured by pulse-chase followed by immunoprecipitation, using an HA tag located at the C terminus of the Ura3 fragment. (B) The fusion proteins used in panel A were tested for their ability to complement the Ura^- phenotype of the host strain by monitoring growth on synthetic complete plates lacking uracil for 2 days at 30°C. (C) Pcl5 tagged at the C terminus with a Myc_3 tag was expressed from the *GAL1* promoter of plasmid KB1030. The stability of the protein was monitored by pulse-chase analysis followed by immunoprecipitation with an anti-Myc antibody. C, no-tag control.

Analysis of the CDS. To test whether the CDS of Pcl5 can function as a portable degradation signal, independently of a cyclin box domain, full-length and progressively shorter C-terminal fragments were fused to the normally stable Ura3 protein. Ura3 activity, as monitored by the ability to complement the growth of a *ura3*Δ strain in the absence of uracil, was abolished when the whole *PCL5* coding sequence was fused C terminally to the *URA3* coding sequence. Progressively shorter C-terminal fragments of Pcl5 lead to intermediate growth phenotypes on uracil-depleted plates (Fig. 3B). The stability of these proteins, as monitored by pulse-chase analysis, revealed that the half-lives of the fusion proteins correlated with URA3 activity (Fig. 3A): Ura3-Pcl5 full-length had the shortest half-life (2.5 min, similar to native Pcl5), whereas the C-terminal 50 amino acids alone led to the protein being degraded with a 5-min half-life, and the last 25 amino acids of Pcl5 alone caused degradation of Pcl5 with a half-life of 15 to 20 min. Ura3 by itself did not display any measurable decay ($t_{1/2} > 30$ min).

These data indicate that the C-terminal 50 amino acids of Pcl5 can function as a degradation signal independently of the rest of the protein. To further characterize this degradation signal, we added a sequence (the Myc_3 epitope) to the C terminus of Pcl5 and followed its degradation. Adding a C-terminal epitope tag to Pcl5 expressed under the *GAL1* promoter led to strong stabilization of the protein (Fig. 3C) compared to the untagged protein (Fig. 2). This result suggests that in order to be effective, the CDS requires a free carboxy terminus.

Analysis of the NDS in overexpressed Pcl5. Since many degradation signals depend on phosphorylation of the protein, we examined the Pcl5 sequence for potential phosphorylation targets. The Pcl5 sequence contains three potential CDK target sites (S/T-P) at positions 8, 32, and 202, of which one, Thr32, is embedded within a Pho85 consensus sequence (TPPL) (Fig. 4A). The threonine residues at these three potential phosphorylation sites were mutated to alanine, individually and in combination. As shown in Fig. 4B, both the triple mutant and the T32A mutant alone showed a moderate extension of the half-life of the protein, from 2.5 to 3 min to 4 min. This weak stabilization was reproduced in several independent experiments. The T8A and T202A mutants, individually or in combination, did not affect Pcl5 stability (data not shown). Since the sequence surrounding Thr32 corresponds to a typical Pho85 consensus sequence, we tested whether Pcl5 degradation depends on Pho85. However, a pulse-chase experiment of Pcl5 expressed from the *CUP1* promoter indicated only marginal stabilization of Pcl5 in the *pho85*Δ strain compared to the wild type (data not shown).

Analysis of Pcl5 NDS at native levels of expression. In the experiments shown above, Pcl5 was overexpressed from strong heterologous promoters. We were concerned that if degradation of Pcl5 via the NDS depends on complex formation with Pho85, then overexpression of Pcl5 might interfere with this degradation pathway by increasing the ratio of uncomplexed versus complexed Pcl5. Pcl5 protein levels are normally very low, probably due to the presence in the *PCL5* mRNA of an extended 5′ untranslated region containing two short open reading frames (S. Aviram, T. Holtzman, and D. Kornitzer, unpublished results). In order to be able to consistently monitor Pcl5 expressed at physiological levels from its native promoter and at the same time to dissociate degradation due to the CDS from N-terminus-dependent degradation, a Myc_{13} tag was integrated at the 3′ end of the chromosomal *PCL5* copy, thereby disabling the CDS, and Pcl5-Myc_{13} levels were monitored by immunoblotting. Comparison of the signal of the Pcl5-Myc_{13} construct with that of Pcl1-Myc_{13} indicated that the former is some 2 orders of magnitude lower (data not shown), i.e., on the order of 10 molecules/cell, based on the calculated cellular amount of Pcl1 (18). Upon addition of the protein synthesis inhibitor cycloheximide, the Pcl5-Myc_{13} protein rapidly disappeared, indicating that at native expression levels, Pcl5 is rapidly degraded even when the C terminus of the protein is blocked with an epitope tag (Fig. 4C). We next tested the effect of the T32A mutation on the levels and stability of natively expressed Pcl5. Wild-type and T32A-mutated Myc_{13}-

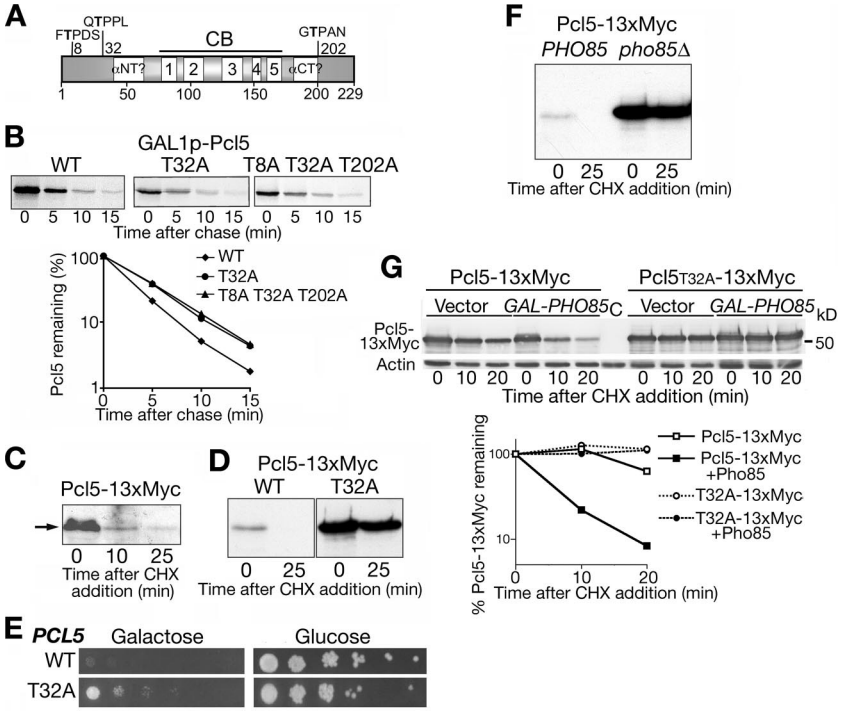

FIG. 4. Role of residue Thr32 and of Pho85 in the degradation of the Pcl5. (A) Location of three putative CDK target sites on Pcl5, with the adjacent sequences. (B) Degradation of *GAL1* promoter-overexpressed Pcl5, wild-type, triply mutated, or singly mutated at Thr32 (plasmids KB1093, KB1236, and KB1222, respectively). Stability of the protein was monitored by pulse-chase analysis, followed by immunoprecipitation with an anti-Pcl5 policlonal antibody. (C) Degradation of natively expressed Pcl5. A Myc_{13} tag was fused to the C terminus of the chromosomal copy of *PCL5* (strain KY1137). The protein was monitored by Western blotting in extracts of growing cells and in extracts treated with the translation inhibitor cycloheximide for the indicated amounts of time. (D) Stability of T32A-mutated, natively expressed Pcl5 tagged with Myc_{13}. Plasmids KB1739 (wild type) and KB1741 (T32A) were used. The membrane was exposed for a shorter time than in panel C to highlight the difference in levels between the wild-type and mutant proteins. (E) The activities of wild-type *PCL5* and *PCL5*(*T32A*) were compared by testing the suppression of Gcn4 overexpression toxicity. The *PCL5* wild-type and mutant genes expressed from their native promoters on plasmids KB1716 and KB1718 were transformed into strain KY827 (*pcl5*Δ). Gcn4 was overexpressed under the *GAL1* promoter of plasmid KB843. Plates were incubated for 3 days at 30°C. (F) Degradation of Myc_{13}-tagged Pcl5 expressed from its native promoter requires Pho85 activity. A chromosomally tagged Pcl5 was visualized as in panel A, in strains KY1137 (wild type) and KY1185 (*pho85*Δ). (G) Degradation of overexpressed, C-terminally tagged Pcl5 requires Thr32 and co-overexpression of Pho85. Pcl5-Myc_{13} and $Pcl5_{T32A}$-Myc_{13} were overexpressed from the *GAL1* promoter of plasmids KB1931 and KB1932, respectively, in the presence of either a vector plasmid or of plasmid KB823, which overexpresses a GST-Pho85 fusion from the *GAL1* promoter. The strains harboring the indicated plasmids were induced in galactose for 3 h. The overexpressed Pcl5-Myc_{13} protein was then monitored by Western blotting in extracts of cells treated with cycloheximide for the indicated amounts of time. The graph represents quantitation of the enhanced chemiluminescence signal of the Pcl5-Myc_{13} bands, normalized for each extract against the actin signal.

tagged *PCL5* were expressed from their native promoters on a centromeric plasmid in a wild-type background. As shown in Fig. 4D, the T32A mutation greatly increased the steady-state levels of the protein and, in contrast to the minor stabilization that the T32A mutation caused with the overexpressed protein, translation inhibition with cycloheximide indicated that the mutant protein expressed from its native promoter was completely stabilized. When natively expressed, the T32A mutant was also significantly more active than the wild type in suppressing Gcn4 overexpression toxicity, as shown in Fig. 4E.

The requirement of Pho85 for degradation of natively expressed Pcl5 was tested by epitope tagging the chromosomal copy of *PCL5* in the *pho85*Δ background. As shown in Fig. 4F, the steady-state levels of Pcl5-Myc_{13} were greatly elevated in the *pho85*Δ mutant versus the wild-type background, and translation inhibition with cycloheximide showed that Pcl5-Myc_{13} is largely stable in the absence of Pho85.

Thr32-dependent degradation of overexpressed Pcl5 can be recovered by co-overexpression of Pho85. C-terminal tagging of Pcl5 with Myc_3 prevented degradation of the protein when overexpressed, probably by inhibiting the CDS (Fig. 3C). In contrast, C-terminal tagging of the natively expressed Pcl5 with Myc_{13} did not prevent degradation (Fig. 4C). We first confirmed that this discrepancy does not represent a peculiarity of the larger tag, by testing the stability of Pcl5-Myc_{13} overexpressed from the *GAL1* promoter. Like with Pcl5-Myc_3 tag, the C-terminally Myc_{13}-tagged protein was largely stable when overexpressed ($t_{1/2} > 20$ min; Fig. 4G). The $Pcl5_{T32A}$-Myc_{13} protein was completely stable, indicating that the residual degradation of overexpressed Pcl5-Myc_{13} depended on Thr32 and confirming that C-terminal tagging inactivates the CDS.

We surmised earlier that Thr32-dependent degradation only takes place when Pcl5 is complexed with its CDK Pho85 and is therefore sensitive to the relative Pcl5-Pho85 stoichiometry. The observation that lowering Pcl5 expression to its native level allowed rapid degradation even when the CDS was inactivated by a C-terminal epitope tag (Fig. 4C) supported this hypothesis. If the relative Pho85-Pcl5 stoichiometry is indeed

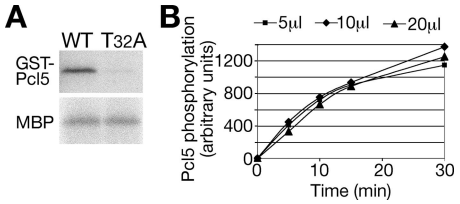

FIG. 5. Pcl5 is phosphorylated on Thr32 by Pho85. (A) The upper panel shows in vitro phosphorylation of GST-Pcl5, either wild-type or mutant T32A, with GST-Pho85. The lower panel shows the same Pho85-Pcl5 recombinant complexes were mixed with myelin basic protein (MBP). See Materials and Methods for the reaction conditions. (B) Kinetics of the same type of Pcl5 phosphorylation reaction shown in panel A. For each time point, 20 ng (each) of GST-Pho85 and GST-Pcl5 were preincubated for 5 min at 30°C and then diluted into increasing volumes of kinase buffer containing 1 μM cold ATP and 1 μCi of [γ-^{32}P]ATP/10 μl. Aliquots were obtained at the indicated times and separated by sodium dodecyl sulfate-polyacrylamide gel electrophoresis, and the GST-Pcl5 label was quantitated with a phosphorimager.

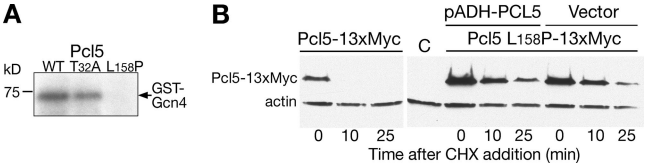

FIG. 6. A catalytically inactive Pcl5 mutant is significantly stabilized. (A) In vitro phosphorylation of GST-Gcn4 with Pho85 and either wild-type Pcl5 or Pcl5 carrying the T32A mutation or inactivating mutation L158P. See Materials and Methods for reaction conditions. (B) Degradation of Myc_{13}-tagged Pcl5 expressed from its native promoter requires cyclin activity. Plasmids carrying the wild-type, 13-Myc-tagged Pcl5 (KB1739) or the inactive Pcl5 L158P (KB1740) were transformed into strain W303, together with either a plasmid expressing wild-type Pcl5 under the strong constitutive *ADH1* promoter (KB1310) or a vector plasmid. Cells were grown at 30°C and treated as for Fig. 5A. Blots were reacted with both anti-Myc antibody (9E10) and anti-actin antibody. C, no-tag control.

important for Thr32-dependent degradation, then, conversely, increasing the levels of the CDK should improve degradation of the overexpressed, C-terminally tagged cyclin. We tested this by overexpressing, together with the *GAL1-PCL5*-Myc_{13} construct, an active GST-Pho85 fusion under the *GAL1* promoter (49). Strikingly, under these conditions, Pcl5-Myc_{13} degradation was in large measure restored ($t_{1/2} < 5$ min; Fig. 4G), whereas the $Pcl5_{T32A}$-Myc_{13} protein was still completely stable, confirming the importance of the CDK-cyclin stoichiometry in Thr32-dependent Pcl5 degradation.

Mechanism of Pcl5 Thr32 phosphorylation. The data shown above are best explained by assuming that Pho85 is responsible for phosphorylation of Pcl5 residue Thr32. We tested this notion directly by reconstituting Thr32 phosphorylation in vitro with purified recombinant proteins. Equal amounts of recombinant GST-Pho85 and GST-Pcl5, either wild type or mutant Thr32Ala, were mixed and reacted in the presence of [γ-^{32}P]ATP. As shown in Fig. 5A (upper panel), a ^{32}P-labeled band that appeared at the position of GST-Pcl5 in the wild-type lane was almost invisible in the Pcl5 Thr32Ala mutant lane. To further ascertain that the two cyclins were otherwise equally active, their activity was tested on the generic CDK substrate myelin basic protein (MBP, lower panel).

The strong dependence of Thr32-dependent degradation on the relative levels of Pcl5 and Pho85 (Fig. 4) suggests that Pcl5 needs to be bound to Pho85 in order to be phosphorylated, i.e., that Pho85 phosphorylates the very cyclin molecule that activates it. A prediction of this model would be that the Pho85-Pcl5 complexes should be phosphorylated with 0th-order kinetics, that is, would not be dependent on concentration. If, on the other hand, the reaction were bimolecular, such that one cyclin-CDK complex phosphorylates another, the kinetics would be predicted to be of second order, i.e., to vary with the square of the concentration. We tested this by measuring the kinetics of the phosphorylation of equal amounts of recombinant Pho85 and Pcl5, diluted in increasing volumes of phosphorylation buffer. As shown in Fig. 5B, the kinetics of phosphorylation remained virtually identical across three twofold dilutions, in accord with 0th-order kinetics.

An additional prediction of the model that each Pcl5 molecule is phosphorylated by the Pho85 molecule that it activates, i.e., *cis*-phosphorylation, is that in vivo, an inactive cyclin mutant should be stable. We isolated a spontaneous missense mutation, Leu158Pro, between the predicted helices IV and V of the Pcl5 cyclin box. The L158P mutant is inactive, as tested by its inability to suppress Gcn4 overexpression toxicity (data not shown) and by its inability to induce Gcn4 phosphorylation by Pho85 in vitro (Fig. 6A). When fused to the Myc_{13} epitope and expressed under its native promoter, this mutant appears strongly stabilized (Fig. 6B). We wanted to further test whether Pcl5 could be phosphorylated in *trans* by Pho85/Pcl5 when Pcl5 is overexpressed. We therefore co-overexpressed wild-type Pcl5 under the strong constitutive *ADH1* promoter, together with Pcl5L158P-Myc_{13}. As shown in Fig. 6B, even overexpression of wild-type Pcl5 did not restore degradation of the Pcl5 L158P mutant cyclin. Overexpression of Pcl5 from the *GAL1* promoter similarly did not restore Pcl5 L158P-Myc_{13} degradation (data not shown). Taken together, these results indicate that the NDS of Pcl5 depends on phosphorylation of residue Thr32 by the Pho85 molecule to which Pcl5 is bound.

Degradation pathway of Pcl5 NDS. Since the SCF ubiquitin ligase is often involved in the degradation of phosphorylated proteins, we tested the stability of Pcl5-Myc_{13} in a mutant of the cullin Cdc53, one of the constant subunits of the SCF complex (63). Even at the semipermissive temperature of 30°C, Pcl5-Myc_{13} was strongly stabilized in the *cdc53-1* mutant (Fig. 7A). Similarly, in the *cdc34-2* strain, mutated in the ubiquitin-conjugating enzyme that collaborates with the SCF complex for substrate ubiquitination, Pcl5-Myc_{13} was strongly stabilized (Fig. 7A). The SCF complex recognizes substrates via the F-box protein subunit (63). We tested Pcl5-Myc_{13} degradation in 14 F-box protein deletion mutants from the EUROSCARF collection, as well as in the *cdc4ts* mutant. Most did not show any effect on degradation of the protein (data not shown). Only deletion of Grr1, an F-box protein required for degradation of G_1 cyclins (2, 58), shows partial stabilization of Pcl5-Myc_{13} (Fig. 7B). This result suggests that the NDS of Pcl5 is recognized by the SCF^{GRR1} ubiquitin ligase; in the absence of Grr1, other F-box proteins may partially stand in for it.

Role of Pcl5 Thr32 phosphorylation in the cellular response to amino acid starvation. Gcn4, the specific target of Pho85/Pcl5, is normally rapidly degraded, but is stabilized upon star-

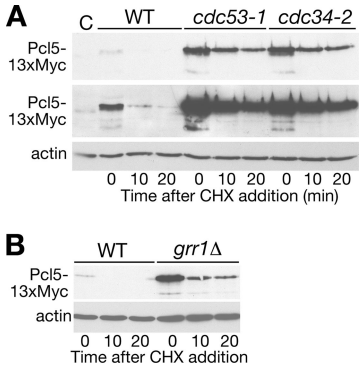

FIG. 7. Degradation of Pcl5 depends on the SCF ubiquitin ligase. The stability of Myc_{13}-tagged Pcl5 expressed from its native promoter (plasmid KB1739) was tested in the SCF mutant *cdc53-1* and in the E2 mutant *cdc34-2* (A) and in the F-box protein mutant *grr1*Δ (B). Cells were grown at 30°C and treated as in Fig. 4C. A second, longer exposure of the anti-Myc reaction is shown in panel A (middle panel) to better visualize Pcl5-Myc_{13} in the wild-type cells. The same blots were reacted with an antiactin antibody to ascertain equal loading (bottom panels).

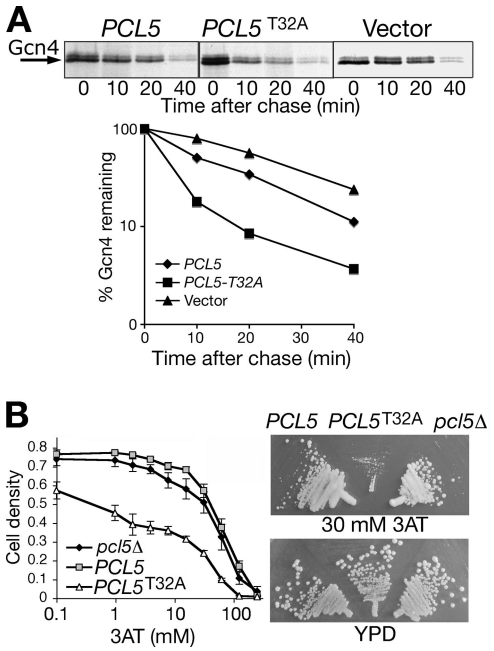

FIG. 8. Effect of Pcl5 mutation T32A on regulation of Gcn4 degradation and amino acid analog resistance. (A) *pcl5*Δ cells (KY827) were transformed with a plasmid overexpressing Myc-tagged Gcn4 (KB1281) and with either a vector plasmid, a plasmid carrying wild-type *PCL5* (KB1716), or a plasmid carrying *PCL5*(*T32A*) (KB1718). The cells were subjected to amino acid starvation for 45 min as previously described (37). Gcn4 decay rate was measured by pulse-chase analysis followed by immunoprecipitation. (B) *pcl5*Δ cells (KY827) transformed with either a vector plasmid, a plasmid carrying wild-type *PCL5* (KB1716), or a plasmid carrying *PCL5*(*T32A*) (KB1718) were grown in synthetic complete medium lacking histidine, with the amino acid analog 3AT. The left panel shows the cell density after overnight growth in liquid medium with increasing 3AT concentrations (mean ± the standard deviation of quadruplicate cultures). The right panel shows growth after 3 days on a 30 mM 3AT plate versus 2 days on a YPD plate.

vation for amino acids (37). The observation that Pcl5 is itself an extremely unstable protein and that its levels drop dramatically in starved cells led us to propose that, by its very instability, Pcl5 functions as a sensor of biosynthetic capacity of the cell: disappearance of Pcl5 under starvation conditions causes stabilization of Gcn4 (56). A prediction of this model is that mutational stabilization of Pcl5 should suppress physiological stabilization of Gcn4 in starved cells. We tested this prediction with the stabilized mutant Pcl5 T32A. As shown in Fig. 8A, in starved cells, Gcn4 degradation was partially inhibited, reaching a half-life of 10 min in cells expressing wild-type Pcl5 (compared to a half-life of 4 min in sated cells; see, for example, Fig. 1D). In contrast, in starved cells expressing Pcl5 T32A, the half-life of Gcn4 was still about 5 min, on the order of the half-life of the protein in sated cells. This suggests that the high metabolic instability of Pcl5 is indeed important for the regulation of Gcn4 stability.

Gcn4 is a key regulator of the cellular response to amino acid starvation (47). We tested the effect of blocking Pcl5 Thr32 phosphorylation on the cellular response to amino acid starvation, by measuring the viability of cells expressing wild-type versus Thr32Ala-mutated Pcl5 in increasing concentrations of 3-aminotriazole (3AT), a histidinol analog that competitively inhibits histidine biosynthesis and is counteracted by elevation of Gcn4 activity (22). We find that even in the absence of 3AT the *PCL5* T32A strain grows more slowly in synthetic complete medium lacking histidine and that the growth defect of this strain is further exacerbated in increasing concentrations of 3AT (Fig. 8B; the derived 3AT 50% inhibitory concentrations were about 60 mM for the wild-type and *pcl5*Δ strains and 22 mM for the T32A strain). Colony growth on histidine-lacking plates containing 30 mM 3AT visually illustrates the growth defect of the *PCL5* T32A strain (Fig. 8B). Thus, Thr32 phosphorylation is important for adequate cellular response to amino acid starvation.

DISCUSSION

Previous studies on cell cycle cyclins, their substrates, and inhibitors suggested that cyclins variously interacted with their substrates via N-terminal (14), C-terminal (26, 35) or cyclin box-located sequences (9, 54, 55). Regarding Pcls, the recently determined structure of the Pho85/Pho80 complex indicates that the Pho80 consists of the core 5-helical cyclin box domain, and an additional αNT, as well as two C-terminal α-helices (αCT1 and αCT2) (30). Huang et al. (30) provide evidence implicating the Pho80 αNT and αCT2 helices in substrate binding. The N-terminal deletions of Pcl5 described here indicated that the predicted α-NT helix region is in fact required for activity. However, a hybrid carrying helices 1 to 5 from Pcl5 and α-NT, as well as the C-terminal helices from Pho80 (80-5-80), functions as Pcl5. This suggests that for Pcl5, unlike the suggested model for Pho80, substrate interaction depends only on the core 5-helix cyclin box domain, whereas the αNT helix plays a distinct, perhaps structural, role. Studies with mammalian cyclin A and with *S. cerevisiae* Clb5 have pointed to a hydrophobic patch on helix 1 of the cyclin box as the site of contact with the substrate or inhibitor (9, 54, 55, 64). Align-

ment of the sequences of fungal Pcl5 orthologs indicates that a sequence of hydrophobic amino acids in the predicted helix1 of the Pcl5 cyclin box is one of the most conserved sites of Pcl5 (our unpublished data). Further experiments will be needed to test whether this region alone can indeed account for the substrate selectivity of Pcl5.

Initial analysis of the degradation signal of Pcl5 painted a complex picture: no single region, when deleted, completely stabilized the protein (our unpublished data), but the addition of C-terminal tags did cause significant stabilization of overexpressed Pcl5. The construction of Pcl5/Pho80 hybrids eventually revealed that Pcl5 contains two distinct degradation signals, an N-terminal, Pho85-dependent signal (NDS) that is active mainly at native levels of expression, and a CDS that is necessary for degradation of overexpressed Pcl5. The presence of two independent degradation signals in Pcl5 may correspond to two distinct Pcl5 pools in the cells: the Pho85-bound and free pools. The CDS is Pho85 independent and would be able to target free Pcl5. At native levels of expression, however, this signal is not essential because Pcl5 can be degraded by the Pho85-dependent, NDS.

Degradation of cell cycle cyclins is dependent on the ubiquitin pathway (21). Since the CDS and NDS do not resemble known cyclin degradation signals, i.e., the APC/cyclosome-dependent destruction box of the mitotic cyclins or the SCF complex-dependent phosphorylated CDSs of G1 cyclins (52, 63), we were interested to identify the degradation systems that recognize those new signals. Regarding the CDS, although we did find that degradation of overexpressed Pcl5 depends on the proteasome (our unpublished data), we were unable to identify ubiquitin pathway mutants that are defective in CDS-dependent degradation. In contrast, we found a strong reduction in NDS-dependent degradation in the SCF mutant *cdc53-1* and in the SCF-associated E2 mutant *cdc34-2*, even under the semipermissive conditions used (30°C), which still allow normal cellular growth and proliferation. All known F-box proteins, representing the substrate recognition subunit of the SCF ubiquitin ligase, were also screened; a partial stabilization was only observed in a strain lacking Grr1, the F-box protein involved in degradation of the G1 cyclin Cln2 (2, 58). Thus, although the possibility that these mutants indirectly affect Pcl5 turnover cannot be entirely dispelled, our results suggest involvement of the SCF ubiquitin ligase, including possibly the Grr1 F-box protein, in targeting the Pcl5 NDS.

We were able to delimit the CDS by deletion analysis to the last 50 amino acids of the protein. The last 25 amino acids did confer instability, but much less than the larger sequence. Interestingly, we find that this signal is inactivated when the C terminus is blocked with the addition of an epitope tag, suggesting that the extreme C terminus is an important part of the signal. We cannot exclude that the actual sequence recognized by the degradation apparatus is much smaller than 50 or even 25 amino acids, but that the extended sequence is required for proper stereochemical configuration of the degradation signal. The role of the CDS is presumably to prevent accumulation of non-Pho85 bound Pcl5 in the cell. Inhibition of the CDS by C-terminal epitope tagging did not show a significant effect on Gcn4 regulation, at least not under conditions of amino acid limitation by addition of the analog 3AT (our unpublished data). Thus, under the conditions tested, the NDS appears to play the dominant role in Pcl5 regulation.

The Pcl5 NDS includes a threonine residue at position 32, which is phosphorylated in the presence of Pho85. We were able to dissociate between degradation via the NDS and the CDS by epitope tagging the C terminus of the protein, thereby inactivating the latter signal. At native levels of expression, Thr32 becomes essential for degradation of Pcl5. The concentration independence of the kinetics of Thr32 phosphorylation in vitro, and the significant stabilization of the inactive mutant L158P in vivo, coupled with the inability to restore degradation of the mutant cyclin by overexpression of wild-type Pcl5 in the cell, together indicate that Thr32 is phosphorylated via a *cis* mechanism, i.e., by the Pho85 molecule that it activates. This mechanism implies that activation of the kinase by Pcl5 is self-limiting: once activated, the CDK will cause phosphorylation of Pcl5 and, once phosphorylated, Pcl5 is subject to rapid degradation. The observation that phosphorylation of a cyclin by its cognate CDK causes its degradation has been made before: degradation of the G1 cyclins Cln3 (66) and Cln2 (38) both depend on phosphorylation on a CDS by their cognate CDK, Cdc28. However, the C-terminal domain of Cln3 alone, in the absence of the cyclin box domain, is phosphorylated and degraded in the presence of active Cdc28 (66), and the C-terminal domain of Cln2 can serve as a portable degradation signal in the absence of the cyclin box domain (5). This implies that in both cases phosphorylation can occur in *trans*, on molecules not bound to the CDK. In contrast, the dependence of Pcl5 degradation on the activity of the cyclin implies a direct link between activation of the CDK and phosphorylation of the bound cyclin, i.e., a *cis* self-catalyzed phosphorylation. This mechanism is supported by the 0th-order reaction kinetics measured in vitro (Fig. 5).

In order to visualize the structural implications of the *cis*-phosphorylation model, the structure of Pcl5 complexed with Pho85 was predicted, based on the resolved Pho85-Pho80 structure (see Materials and Methods). In this predicted structure (Fig. 9), Thr32 (red spheres) is found at a significant distance (ca. 40 Å) from the Pho85 catalytic cleft (which is located underneath the bound ATP). It should be noted that the extreme N terminus of the depicted Pcl5 sequence—residues 26 to 40 (shown in red)—could not be modeled due to limited homology to Pho80, and furthermore, the whole N terminus of Pcl5 (residues 1 to 40) is predicted to be disordered (31). However, even assuming significant extension of the disordered region toward the Pho85 catalytic cleft, the distance may be too large to be bridged without additional conformational changes in the N terminus, e.g., rotation around one of several hinges that are predicted (17) to occur in the N-terminal helix (light green). The notion of a requirement for a significant conformation change in order to allow Thr32 phosphorylation is in agreement with the relatively slow kinetics of the reaction even after the Pho85-Pcl5 complex is formed (Fig. 5).

The *cis* versus *trans* mechanisms have important implications with regard to the kinetics of the phosphorylation reaction in vivo. In the *trans* case, the rate of phosphorylation is dependent on the square of the cellular concentration of the cyclin-CDK complex. Thus, for cyclically expressed cyclins, protein concentration may be allowed to build up until a certain threshold is

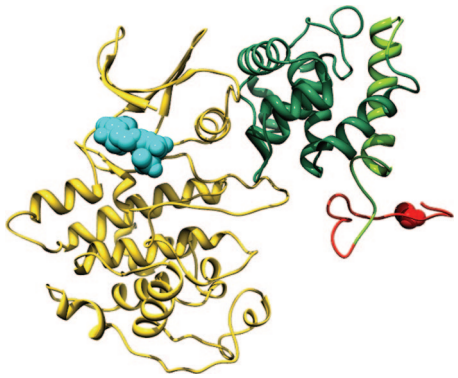

FIG. 9. Predicted Pcl5-Pho85 structure. The model includes the Pho85 structure (2pmi [30]) and Pcl5 (residues 26 to 189) modeled after Pho80 (see Materials and Methods for the modeling protocol). Pho85 is colored in yellow, and the ATP analogue ATP-γ-S is depicted as blue spheres. The Pcl5 cyclin box domain (residues 75 to 189) is colored dark green, the N-terminal domain including helix αNT (residues 41 to 74) is colored light green, and residues 26 to 40, predicted to be disordered, are colored red. Thr32 is shown as red spheres. The image was produced by using the Chimera package (University of California at San Francisco).

reached, beyond which phosphorylation and degradation are greatly increased. In contrast, in the *cis* case, phosphorylation and degradation are only dependent on the rate of complex formation with the CDK, ensuring that the active cyclin-CDK complex has a limited lifetime at all levels of cyclin. This mechanism may be essential to ensure the degradation of a cyclin like Pcl5, which is normally present at very low levels.

We had previously suggested that high turnover of Pcl5 is important for the regulation of Gcn4 stability: the high metabolic instability of Pcl5 causes it to rapidly disappear from the cells under starvation conditions, leading to stabilization of Gcn4 (56). This model predicts that stabilization of Pcl5 should cause constitutive degradation of Gcn4. Recently, an alternative model was proposed, that the Pho85-Pcl5 interaction is reduced under starvation conditions, via a mechanism that remains to be elucidated (6). Here, we tested the prediction that metabolic instability of Pcl5 is important for the proper response to amino acid starvation conditions, by measuring the stability of Gcn4 and 3AT resistance in cells expressing the *PCL5*(*T32A*) allele. These responses are indeed defective in the presence of the mutant allele, providing support for the former model. The mechanism of self-catalyzed phosphorylation of the Pcl5 cyclin, implying a self-contained timing mechanism for its own demise, buttresses the suggested role of Pcl5 as sensor of the biosynthetic capacity of the cell within the pathway of regulation of Gcn4 turnover.

The mammalian CDK5 activator p35, the structural homolog of Pho80 and, presumably, of Pcl5, is rapidly turned over in a manner dependent on CDK5 activity (50). N-terminal truncation of p35 yields a stabilized, hyperactive protein species, p25, that is associated with several neurodegenerative diseases (50, 51; reviewed in reference 12). Here, we identified a Pho85 phosphorylation site in the N terminus of Pcl5 that causes degradation of the cyclin and is necessary for adequate response to amino acid starvation. We propose that homologous mechanisms, including phosphorylation in *cis* by the cognate CDK, may keep the activities of Pcl5 and of the cyclin-like protein p35 in check.

ACKNOWLEDGMENTS

We thank Brenda Andrews, Erin O'Shea, Mike Tyers, Masafumi Nishizawa, and Dick Kulka for plasmids and strains; Yael Mandel-Gutfreund for advice with protein structure prediction; and Sara Selig for critical reading of the manuscript.

This research project was supported by grants from the Israel Science Foundation and the Niedersachsen-Israel Volkswagen Foundation. The Chimera package from the Computer Graphics Laboratory, University of California, San Francisco, is supported by NIH P41 RR-01081.

REFERENCES

1. **Altschul, S. F., T. L. Madden, A. A. Schaffer, J. Zhang, Z. Zhang, W. Miller, and D. J. Lipman.** 1997. Gapped BLAST and PSI-BLAST: a new generation of protein database search programs. Nucleic Acids Res. **25:**3389–3402.
2. **Barral, Y., S. Jentsch, and C. Mann.** 1995. G1 cyclin turnover and nutrient uptake are controlled by a common pathway in yeast. Genes Dev. **9:**399–409.
3. **Belle, A., A. Tanay, L. Bitincka, R. Shamir, and E. K. O'Shea.** 2006. Quantification of protein half-lives in the budding yeast proteome. Proc. Natl. Acad. Sci. USA **103:**13004–13009.
4. **Berman, H. M., J. Westbrook, Z. Feng, G. Gilliland, T. N. Bhat, H. Weissig, I. N. Shindyalov, and P. E. Bourne.** 2000. The Protein Data Bank. Nucleic Acids Res. **28:**235–242.
5. **Berset, C., P. Griac, R. Tempel, J. La Rue, C. Wittenberg, and S. Lanker.** 2002. Transferable domain in the G(1) cyclin Cln2 sufficient to switch degradation of Sic1 from the E3 ubiquitin ligase SCF(Cdc4) to SCF(Grr1). Mol. Cell. Biol. **22:**4463–4476.
6. **Bomeke, K., R. Pries, V. Korte, E. Scholz, B. Herzog, F. Schulze, and G. H. Braus.** 2006. Yeast Gcn4p stabilization is initiated by the dissociation of the nuclear Pho85p/Pcl5p complex. Mol. Biol. Cell. **17:**2952–2962.
7. **Bregman, D. B., R. G. Pestell, and V. J. Kidd.** 2000. Cell cycle regulation and RNA polymerase II. Front. Biosci. **5:**D244–D257.
8. **Brown, N. R., M. E. Noble, J. A. Endicott, E. F. Garman, S. Wakatsuki, E. Mitchell, B. Rasmussen, T. Hunt, and L. N. Johnson.** 1995. The crystal structure of cyclin A. Structure **3:**1235–1247.
9. **Brown, N. R., M. E. Noble, J. A. Endicott, and L. N. Johnson.** 1999. The structural basis for specificity of substrate and recruitment peptides for cyclin-dependent kinases. Nat. Cell Biol. **1:**438–443.
10. **Carroll, A. S., and E. K. O'Shea.** 2002. Pho85 and signaling environmental conditions. Trends Biochem. Sci. **27:**87–93.
11. **Chi, Y., M. J. Huddleston, X. Zhang, R. A. Young, R. S. Annan, S. A. Carr, and R. J. Deshaies.** 2001. Negative regulation of Gcn4 and Msn2 transcription factors by Srb10 cyclin-dependent kinase. Genes Dev. **15:**1078–1092.
12. **Cruz, J. C., and L. H. Tsai.** 2004. A Jekyll and Hyde kinase: roles for Cdk5 in brain development and disease. Curr. Opin. Neurobiol. **14:**390–394.
13. **Dohmen, R. J., K. Madura, B. Bartel, and A. Varshavsky.** 1991. The N-end rule is mediated by the UBC2(RAD6) ubiquitin-conjugating enzyme. Proc. Natl. Acad. Sci. USA **88:**7351–7355.
14. **Dowdy, S. F., P. W. Hinds, K. Louie, S. I. Reed, A. Arnold, and R. A. Weinberg.** 1993. Physical interaction of the retinoblastoma protein with human D cyclins. Cell **73:**499–511.
15. **Eswar, N., D. Eramian, B. Webb, M. Y. Shen, and A. Sali.** 2008. Protein structure modeling with MODELLER. Methods Mol. Biol. **426:**145–159.
16. **Evans, T., E. T. Rosenthal, J. Youngblom, D. Distel, and T. Hunt.** 1983. Cyclin: a protein specified by maternal mRNA in sea urchin eggs that is destroyed at each cleavage division. Cell **33:**389–396.
17. **Flores, S. C., K. S. Keating, J. Painter, F. Morcos, K. Nguyen, E. A. Merritt, L. A. Kuhn, and M. B. Gerstein.** 2008. HingeMaster: normal mode hinge prediction approach and integration of complementary predictors. Proteins **73:**299–319.
18. **Ghaemmaghami, S., W. K. Huh, K. Bower, R. W. Howson, A. Belle, N. Dephoure, E. K. O'Shea, and J. S. Weissman.** 2003. Global analysis of protein expression in yeast. Nature **425:**737–741.
19. **Gildor, T., R. Shemer, A. Atir-Lande, and D. Kornitzer.** 2005. Coevolution of cyclin pcl5 and its substrate gcn4. Eukaryot. Cell **4:**310–318.
20. **Gilon, T., O. Chomsky, and R. G. Kulka.** 1998. Degradation signals for ubiquitin system proteolysis in *Saccharomyces cerevisiae*. EMBO J. **17:**2759–2766.
21. **Glotzer, M., A. W. Murray, and M. W. Kirschner.** 1991. Cyclin is degraded by the ubiquitin pathway. Nature **349:**132–138.
22. **Hinnebusch, A. G.** 1992. General and pathway-specific regulatory mechanisms controlling the synthesis of amino acid biosynthetic enzymes in *Saccharomyces cerevisiae*, p. 319–414. *In* E. W. Jones, J. R. Pringle, and J. R. Broach (ed.), The molecular and cellular biology of the yeast *Saccharomyces*, vol. 2. Cold Spring Harbor Laboratory Press, Plainview, NY.

23. **Hinnebusch, A. G., and G. R. Fink.** 1983. Positive regulation in the general control of *Saccharomyces cerevisiae*. Proc. Natl. Acad. Sci. USA **80:**5374–5378.
24. **Hirst, K., F. Fisher, P. C. McAndrew, and C. R. Goding.** 1994. The transcription factor, the Cdk, its cyclin and their regulator: directing the transcriptional response to a nutritional signal. EMBO J. **13:**5410–5420.
25. **Hope, I. A., and K. Struhl.** 1985. GCN4 protein, synthesized in vitro, binds HIS3 regulatory sequences: implications for general control of amino acid biosynthetic genes in yeast. Cell **43:**177–188.
26. **Horton, L. E., and D. J. Templeton.** 1997. The cyclin box and C terminus of cyclins A and E specify CDK activation and substrate specificity. Oncogene **14:**491–498.
27. **Huang, D., H. Friesen, and B. Andrews.** 2007. Pho85, a multifunctional cyclin-dependent protein kinase in budding yeast. Mol. Microbiol. **66:**303–314.
28. **Huang, D., J. Moffat, W. A. Wilson, L. Moore, C. Cheng, P. J. Roach, and B. Andrews.** 1998. Cyclin partners determine Pho85 protein kinase substrate specificity in vitro and in vivo: control of glycogen biosynthesis by Pcl8 and Pcl10. Mol. Cell. Biol. **18:**3289–3299.
29. **Huang, D., G. Patrick, J. Moffat, L. H. Tsai, and B. Andrews.** 1999. Mammalian Cdk5 is a functional homologue of the budding yeast Pho85 cyclin-dependent protein kinase. Proc. Natl. Acad. Sci. USA **96:**14445–14450.
30. **Huang, K., I. Ferrin-O'Connell, W. Zhang, G. A. Leonard, E. K. O'Shea, and F. A. Quiocho.** 2007. Structure of the Pho85-Pho80 CDK-cyclin complex of the phosphate-responsive signal transduction pathway. Mol. Cell **28:**614–623.
31. **Ishida, T., and K. Kinoshita.** 2008. Prediction of disordered regions in proteins based on the meta approach. Bioinformatics **24:**1344–1348.
32. **Jeffrey, P. D., A. A. Russo, K. Polyak, E. Gibbs, J. Hurwitz, J. Massague, and N. P. Pavletich.** 1995. Mechanism of CDK activation revealed by the structure of a cyclinA-CDK2 complex. Nature **376:**313–320.
33. **Jones, D. T.** 1999. Protein secondary structure prediction based on position-specific scoring matrices. J. Mol. Biol. **292:**195–202.
34. **Kaffman, A., I. Herskowitz, R. Tjian, and E. K. O'Shea.** 1994. Phosphorylation of the transcription factor PHO4 by a cyclin-CDK complex, PHO80-PHO85. Science **263:**1153–1156.
35. **Kelly, B. L., K. G. Wolfe, and J. M. Roberts.** 1998. Identification of a substrate-targeting domain in cyclin E necessary for phosphorylation of the retinoblastoma protein. Proc. Natl. Acad. Sci. USA **95:**2535–2540.
36. **Kornitzer, D.** 2002. Monitoring protein degradation. Methods Enzymol. **351:**639–647.
37. **Kornitzer, D., B. Raboy, R. G. Kulka, and G. R. Fink.** 1994. Regulated degradation of the transcription factor Gcn4. EMBO J. **13:**6021–6030.
38. **Lanker, S., M. H. Valdivieso, and C. Wittenberg.** 1996. Rapid degradation of the G1 cyclin Cln2 induced by CDK-dependent phosphorylation. Science **271:**1597–1601.
39. **Longtine, M. S., A. McKenzie III, D. J. Demarini, N. G. Shah, A. Wach, A. Brachat, P. Philippsen, and J. R. Pringle.** 1998. Additional modules for versatile and economical PCR-based gene deletion and modification in *Saccharomyces cerevisiae*. Yeast **14:**953–961.
40. **Measday, V., L. Moore, R. Retnakaran, J. Lee, M. Donoviel, A. M. Neiman, and B. Andrews.** 1997. A family of cyclin-like proteins that interact with the Pho85 cyclin-dependent kinase. Mol. Cell. Biol. **17:**1212–1223.
41. **Meimoun, A., T. Holtzman, Z. Weissman, H. J. McBride, D. J. Stillman, G. R. Fink, and D. Kornitzer.** 2000. Degradation of the transcription factor Gcn4 requires the kinase Pho85 and the SCF(CDC4) ubiquitin-ligase complex. Mol. Biol. Cell **11:**915–927.
42. **Meng, E. C., E. F. Pettersen, G. S. Couch, C. C. Huang, and T. E. Ferrin.** 2006. Tools for integrated sequence-structure analysis with UCSF Chimera. BMC Bioinform. **7:**339.
43. **Miller, M. E., and F. R. Cross.** 2001. Cyclin specificity: how many wheels do you need on a unicycle? J. Cell Sci. **114:**1811–1820.
44. **Morgan, D. O.** 1995. Principles of CDK regulation. Nature **374:**131–134.
45. **Mumberg, D., R. Muller, and M. Funk.** 1994. Regulatable promoters of *Saccharomyces cerevisiae*: comparison of transcriptional activity and their use for heterologous expression. Nucleic Acids Res. **22:**5767–5768.
46. **Nasmyth, K.** 2001. A prize for proliferation. Cell **107:**689–701.
47. **Natarajan, K., M. R. Meyer, B. M. Jackson, D. Slade, C. Roberts, A. G. Hinnebusch, and M. J. Marton.** 2001. Transcriptional profiling shows that Gcn4p is a master regulator of gene expression during amino acid starvation in yeast. Mol. Cell. Biol. **21:**4347–4368.
48. **Nishizawa, M., Y. Kanaya, and E. A. Toh.** 1999. Mouse cyclin-dependent kinase (Cdk) 5 is a functional homologue of a yeast Cdk, Pho85 kinase. J. Biol. Chem. **274:**33859–33862.
49. **Nishizawa, M., M. Kawasumi, M. Fujino, and A. Toh-e.** 1998. Phosphorylation of sic1, a cyclin-dependent kinase (Cdk) inhibitor, by Cdk including Pho85 kinase is required for its prompt degradation. Mol. Biol. Cell **9:**2393–2405.
50. **Patrick, G. N., P. Zhou, Y. T. Kwon, P. M. Howley, and L. H. Tsai.** 1998. p35, the neuronal-specific activator of cyclin-dependent kinase 5 (Cdk5) is degraded by the ubiquitin-proteasome pathway. J. Biol. Chem. **273:**24057–24064.
51. **Patrick, G. N., L. Zukerberg, M. Nikolic, S. de la Monte, P. Dikkes, and L. H. Tsai.** 1999. Conversion of p35 to p25 deregulates Cdk5 activity and promotes neurodegeneration. Nature **402:**615–622.
52. **Peters, J. M.** 2002. The anaphase-promoting complex: proteolysis in mitosis and beyond. Mol. Cell **9:**931–943.
53. **Pettersen, E. F., T. D. Goddard, C. C. Huang, G. S. Couch, D. M. Greenblatt, E. C. Meng, and T. E. Ferrin.** 2004. UCSF Chimera: a visualization system for exploratory research and analysis. J. Comput. Chem. **25:**1605–1612.
54. **Russo, A. A., P. D. Jeffrey, A. K. Patten, J. Massague, and N. P. Pavletich.** 1996. Crystal structure of the $p27^{Kip1}$ cyclin-dependent-kinase inhibitor bound to the cyclin A-Cdk2 complex. Nature **382:**325–331.
55. **Schulman, B. A., D. L. Lindstrom, and E. Harlow.** 1998. Substrate recruitment to cyclin-dependent kinase 2 by a multipurpose docking site on cyclin A. Proc. Natl. Acad. Sci. USA **95:**10453–10458.
56. **Shemer, R., A. Meimoun, T. Holtzman, and D. Kornitzer.** 2002. Regulation of the transcription factor Gcn4 by Pho85 cyclin PCL5. Mol. Cell. Biol. **22:**5395–5404.
57. **Sikorski, R. S., and P. Hieter.** 1989. A system of shuttle vectors and yeast host strains designed for efficient manipulation of DNA in *Saccharomyces cerevisiae*. Genetics **122:**19–27.
58. **Skowyra, D., D. M. Koepp, T. Kamura, M. N. Conrad, R. C. Conaway, J. W. Conaway, S. J. Elledge, and J. W. Harper.** 1999. Reconstitution of G1 cyclin ubiquitination with complexes containing SCFGrr1 and rbx1. Science **284:**662–665.
59. **Soding, J.** 2005. Protein homology detection by HMM-HMM comparison. Bioinformatics **21:**951–960.
60. **Tarricone, C., R. Dhavan, J. Peng, L. B. Areces, L. H. Tsai, and A. Musacchio.** 2001. Structure and regulation of the CDK5-p25(nck5a) complex. Mol. Cell **8:**657–669.
61. **Tavernarakis, N., and G. Thireos.** 1995. Transcriptional interference caused by GCN4 overexpression reveals multiple interactions mediating transcriptional activation. Mol. Gen. Genet. **247:**571–578.
62. **Toh-e, A., Y. Ueda, S. I. Kakimoto, and Y. Oshima.** 1973. Isolation and characterization of acid phosphatase mutants in *Saccharomyces cerevisiae*. J. Bacteriol. **113:**727–738.
63. **Willems, A. R., M. Schwab, and M. Tyers.** 2004. A hitchhiker's guide to the cullin ubiquitin ligases: SCF and its kin. Biochim. Biophys. Acta **1695:**133–170.
64. **Wilmes, G. M., V. Archambault, R. J. Austin, M. D. Jacobson, S. P. Bell, and F. R. Cross.** 2004. Interaction of the S-phase cyclin Clb5 with an "RXL" docking sequence in the initiator protein Orc6 provides an origin-localized replication control switch. Genes Dev. **18:**981–991.
65. **Wilson, W. A., A. M. Mahrenholz, and P. J. Roach.** 1999. Substrate targeting of the yeast cyclin-dependent kinase Pho85p by the cyclin Pcl10p. Mol. Cell. Biol. **19:**7020–7030.
66. **Yaglom, J., H. K. Linskens, S. Sadis, D. M. Rubin, B. Futcher, and D. Finley.** 1995. p34-Cdc28-mediated control of Cln3 degradation. Mol. Cell. Biol. **15:**731–741.
67. **Yoshida, K., N. Ogawa, and Y. Oshima.** 1989. Function of the PHO regulatory genes for repressible acid phosphatase synthesis in *Saccharomyces cerevisiae*. Mol. Gen. Genet. **217:**40–46.
68. **Zachariae, W., and K. Nasmyth.** 1999. Whose end is destruction: cell division and the anaphase-promoting complex. Genes Dev. **13:**2039–2058.